ARL-TR-9060 ● SEP 2020

DEVCOM ARMY RESEARCH LABORATORY

In-situ Atmospheric Intelligence for Hybrid Power Grids: Volume 2 (Automated Data Flow Tests)

by Gail Vaucher, Morris Berman, Gordon Parker, Michael Lee, Sean D'Arcy, Robert Jane, and Thomas Price

Approved for public release; distribution is unlimited.

NOTICES

Disclaimers

The findings in this report are not to be construed as an official Department of the Army position unless so designated by other authorized documents.

Citation of manufacturer's or trade names does not constitute an official endorsement or approval of the use thereof.

Destroy this report when it is no longer needed. Do not return it to the originator.

ARL-TR-9060 ● SEP 2020

In-situ Atmospheric Intelligence for Hybrid Power Grids: Volume 2 (Automated Data Flow Tests)

Gail Vaucher, Michael Lee, and Sean D'Arcy
Computational and Information Sciences Directorate, CCDC Army Research Laboratory

Morris Berman and Robert Jane
Sensors and Electron Devices Directorate, CCDC Army Research Laboratory

Gordon Parker and Thomas Price
Michigan Technology University

Approved for public release; distribution is unlimited.

REPORT DOCUMENTATION PAGE			Form Approved OMB No. 0704-0188

Public reporting burden for this collection of information is estimated to average 1 hour per response, including the time for reviewing instructions, searching existing data sources, gathering and maintaining the data needed, and completing and reviewing the collection information. Send comments regarding this burden estimate or any other aspect of this collection of information, including suggestions for reducing the burden, to Department of Defense, Washington Headquarters Services, Directorate for Information Operations and Reports (0704-0188), 1215 Jefferson Davis Highway, Suite 1204, Arlington, VA 22202-4302. Respondents should be aware that notwithstanding any other provision of law, no person shall be subject to any penalty for failing to comply with a collection of information if it does not display a currently valid OMB control number.
PLEASE DO NOT RETURN YOUR FORM TO THE ABOVE ADDRESS.

1. REPORT DATE *(DD-MM-YYYY)*	2. REPORT TYPE	3. DATES COVERED (From - To)
September 2020	Technical Report	1 October 2019–30 September 2020

4. TITLE AND SUBTITLE	5a. CONTRACT NUMBER
In-situ Atmospheric Intelligence for Hybrid Power Grids: Volume 2 (Automated Data Flow Tests)	5b. GRANT NUMBER
	5c. PROGRAM ELEMENT NUMBER

6. AUTHOR(S)	5d. PROJECT NUMBER
Gail Vaucher, Morris Berman, Gordon Parker, Michael Lee, Sean D'Arcy, Robert Jane, and Thomas Price	5e. TASK NUMBER
	5f. WORK UNIT NUMBER

7. PERFORMING ORGANIZATION NAME(S) AND ADDRESS(ES)	8. PERFORMING ORGANIZATION REPORT NUMBER
CCDC Army Research Laboratory ATTN: FCDD-RLC-ED White Sands Missile Range, NM 88002-5501	ARL-TR-9060

9. SPONSORING/MONITORING AGENCY NAME(S) AND ADDRESS(ES)	10. SPONSOR/MONITOR'S ACRONYM(S)
	11. SPONSOR/MONITOR'S REPORT NUMBER(S)

12. DISTRIBUTION/AVAILABILITY STATEMENT
Approved for public release; distribution is unlimited.

13. SUPPLEMENTARY NOTES
ORCID IDs: Robert Jane, 0000-0001-6742-7306; Michael Lee, 0000-0002-0419-6069

14. ABSTRACT
Uninterrupted electrical power is critical to current and future successes of the armed services. Future Multi-Domain Operations battlefields will be filled with multiple dissimilar energy networks. To achieve battlespace dominance, energy flow characterizations of individual platforms and the aggregate battlespace must be developed to adapt and exploit the variable operating conditions. The Atmospheric Intelligence for Hybrid Power Grids (AI-HPG) Project goals seek to develop and demonstrate the ability to use organically obtained atmospheric knowledge to forecast and optimize a hybridized grid's short-term energy requirements. The current effort focuses on effectively integrating photovoltaics, as a local energy source, into traditional power resources for demonstration purposes. Once successful, a wide range of locally sourced energy sources could follow. This project focused on investigating an AIHPG Test-bed that would generate data that could prove/disprove the feasibility of integrated, tactical hybrid power and provide additional real-world measurements useful to future simulation work. In Phase I, a tactical hybrid power simulation with atmospheric input was constructed. Phase II proved the feasibility of the simulation. This report documents Phase III's success in automating the AI-HPG Test-bed, which consists of three major components: atmospheric intelligence, power optimization, and coincident data acquired to calibrate AI-HPG Testbed components.

15. SUBJECT TERMS
hybrid power grid, power optimization, PV, atmospheric intelligence, machine learning, solar radiation, sky image analyses

16. SECURITY CLASSIFICATION OF:			17. LIMITATION OF ABSTRACT	18. NUMBER OF PAGES	19a. NAME OF RESPONSIBLE PERSON
a. REPORT	b. ABSTRACT	c. THIS PAGE			Gail Vaucher
Unclassified	Unclassified	Unclassified	UU	52	19b. TELEPHONE NUMBER (Include area code) (575) 678-2334

Standard Form 298 (Rev. 8/98)
Prescribed by ANSI Std. Z39.18

Contents

List of Figures v

Acknowledgments vii

Executive Summary viii

1. Introduction 1

2. System Design 7

2.1 Long-Term Vision 8

2.2 Short-Term Vision 8

3. System Elements 9

3.1 Hardware 9

3.2 Automating Script 10

3.3 Sensor Data 14

3.3.1 Panel Temperature 14

3.3.2 WSI 14

3.3.3 Validation Data 15

3.4 Whole Sky Image Analyses 15

3.5 Solar Radiation Model 17

3.6 Power Conversion 19

3.7 Power Optimization 19

3.7.1 Integrating the AI-HPG Optimization Function 19

3.7.2 AI-HPG Optimization Input 19

3.7.3 Optimization Routine 20

3.8 AI-HPG Test-bed Emulator 22

4. Data Flow Tests 22

4.1 Data Flow Test #1 23

4.2 Data Flow Test #2 23

5. Lessons Learned (by Element) 24

5.1 Hardware 24

5.2 Automating Script 24

5.3 Sensor Data 25

5.4 Validation Data 25

5.5 Whole Sky Image Analyses 25

5.6 Solar Radiation Model 25

5.7 Power Conversion 26

5.8 Optimization 26

5.9 Test-bed Emulator 26

6. Future Vision 27

7. Results and Conclusion 27

8. References 28

Appendix A. Atmospheric Intelligence for Hybrid Power Grids (AI-HPG) Data Flow Test #1: Quasi-automated Element Checks 29

Appendix B. Atmospheric Intelligence for Hybrid Power Grids (AI-HPG) Data Flow Test #2: Automating the Process 34

List of Symbols, Abbreviations, and Acronyms 39

Distribution List 40

List of Figures

Fig. 1 Example microgrid electrical load profile 2

Fig. 2 Example atmospheric conditions 2

Fig. 3 Example fuel consumption characteristics 3

Fig. 4 No atmospheric knowledge case results: PV and energy storage power requirements. (The sign of the PV and storage power are opposite; positive indicates that the PV array is supplying power, while positive storage power indicates that the storage is charging. Similarly, negative storage power indicates that the storage is discharging.) 3

Fig. 5 No atmospheric knowledge case results: diesel generator power requirements 3

Fig. 6 No atmospheric knowledge case results: fuel consumption and energy storage performance metrics 4

Fig. 7 Current atmospheric knowledge case results: PV and energy storage power requirements. (PV and storage power signs are opposite; positive indicates that the PV array is supplying power, while positive storage power indicates that the storage is charging. Similarly, negative storage power indicates that the storage is discharging.) 4

Fig. 8 Current atmospheric knowledge case results: diesel generator power requirements 5

Fig. 9 Current atmospheric knowledge case results: fuel consumption and energy storage performance metrics 5

Fig. 10 Current and future atmospheric knowledge case results: PV and energy storage power requirements. (The sign of the PV and storage power are opposite; positive indicates that the PV array is supplying power, while positive storage power indicates that the storage is charging. Similarly, negative storage power indicates that the storage is discharging.) 6

Fig. 11 Current and future atmospheric knowledge case results: diesel generator power requirements 6

Fig. 12 Current and future atmospheric knowledge case results: fuel consumption and energy storage performance metrics 7

Fig. 13 Original AI-HPG Test-bed showing the design. Miniature WSI (not shown here) replaced the original simulated-WSI Camera System in 2020 10

Fig. 14 Executive object structure 12

Fig. 15 Execute object loop flow 13

Fig. 16 a) Original partly cloudy WSI image; b) ML predictions on a); c) original clear sky image; and d) ML predictions on c) 17

Fig. 17 Graphical user interface for the Solar Radiation Flux model input with graphed output 18
Fig. 18 Typical 24-h, fuel-optimal generator solution provided by the EMS in response to inputs from the supervisory controller running on the AI-HPG Platform 21
Fig. A-1 Whole sky imager image used for AI-HPG Data Flow Test #1 represented a Clear Sky Case, from 2019 September 18, at 1200 MT 31
Fig. A-2 Data Flow Test #1, WSI analysis output sent to the operating platform 31
Fig. A-3 SR model GUI, showing the AI-HPG Data Flow Test #1, 2019 September 18 input and output 32
Fig. A-4 SR model data calculated for 2019 September 18 32
Fig. A-5 2019 September 18 Panel Power and pGen output data from the AI-HPG Data Flow Test #1 conducted on 2020 June 03 33
Fig. B-1 AI-HPG Data Flow Test #2c results for 2019 August 19, 1245 MT .. 37
Fig. B-2 AI-HPG Data Flow Test #2c results for 2019 August 19, 1300 MT .. 38
Fig. B-3 AI-HPG Data Flow Test #2c results for 2019 August 19, 1315 MT .. 38
Fig. B-4 AI-HPG Data Flow Test #2c results for 2019 August 19, 1330 MT .. 38

Acknowledgments

The authors wish to thank Mr Robert Brice for his work with the Atmospheric Intelligence for Hybrid Power Grids (AI-HPG) pyranometers; the Army Test and Evaluation Command - Meteorology Department (Mr Blaine Thomas) for their support during our temporary relocation requirement; and the computer administrative personnel who assisted in setting up the common AI-HPG Platform that facilitates this multiple-organization project. Finally, a special thanks go to the Technical Publishing Branch for its technical editing excellence, specifically to Ms Nancy Simini and Ms Jessica Schultheis.

Executive Summary

Providing uninterrupted electrical power is critical to current and future successes of the US Armed Services. Future Multi-Doman Operations battlefields will be filled with multiple dissimilar energy networks. This chaotic operational environment will be limited by variable operating conditions (mission profiles, terrain, atmospheric conditions), copious amounts of real-time actionable intelligence derived from weapon and sensor suites, and most importantly, the energy capabilities of each platform. To achieve battlespace dominance, energy flow characterizations of individual platforms and the aggregate battlespace must be developed with respect to the variable operating conditions.

This study marks one of several steps toward bridging the gap between contemporary electrical power capabilities and the ideals of the future, when a diversity of integrated tactical power resources has become "the norm" and the performance of these multiple resources flawlessly provides uninterrupted electrical power for a multitude of platforms. While the study's design is geared for tactical applications, this research is equally applicable to emergency power applications, such as those following natural disasters.

The Atmospheric Intelligence for Hybrid Power Grids (AI-HPG) Project long-term goals seek to develop and demonstrate the ability to utilize organically obtained atmospheric knowledge to forecast and optimize a hybridized grid's short-term energy needs and availability. The current effort focuses on effectively integrating photovoltaics as a local energy source into traditional power resources, for demonstration purposes. Once successful, a wide range of locally sourced energy resources could follow, such as hydroelectric, wind, geothermal, as well as foraged energy sources.

This research study has evolved in phases. In Phase I, the not-yet-constructed hybridized grid was simulated. After demonstrating a fuel reduction when atmospheric intelligence was introduced into the grid-optimizing routine, Phase II pursued current and locally forecasted atmospheric intelligence contributing to the power distribution strategies. The "in-situ (local) resources only" restriction provided a novel framework for the study's tactical and disaster relief applications. Phase II also raised the question regarding whether the simulation work could be proven in a real-world setting.

Phase III answered with a goal of creating an automated AI-HPG Test-bed demonstration. The construction of the AI-HPG Test-bed would 1) generate data that could prove/disprove the feasibility of the integrated, simulated hybrid power and 2) provide additional real-world measurements useful to future simulation

work. Concurrent with the proposed employment of artificial intelligence and machine learning research techniques within this study, came a need for significantly larger data resources. The AI-HPG Test-bed had the potential for becoming just such a healthy real-world power and atmospheric data resource.

The AI-HPG Test-bed design consists of three major components: the atmospheric intelligence, the power optimization, and coincident data acquired to calibrate AI-HPG Test-bed components. The designed data flow sequence by major components follows.

1. Atmospheric Intelligence Component
    1.1 Panel Temperature Acquisition
    1.2 Solar Radiation Calculation
        1.2.1 Whole Sky Imager Image Acquisition
        1.2.2 Whole Sky Imager Image Analysis
        1.2.3 Solar radiation model calculates current and future solar radiation
2. Power Optimization Component
    2.1 Power Conversion
    2.2 Power Optimization
    2.3 Integrated optimization solution into the emulated AI-HPG Test-bed
3. Data for Model Improvements
    3.1 Pyranometer data acquired to improve solar radiation method
    3.2 Power Train data acquired to improve optimization routines

Within this technical report, each of the AI-HPG Test-bed elements are described (Section 3). In Section 4, an overview of the two Data Flow Tests is summarized. (Note: Due to 2019 Corona Virus Infectious Disease (COVID-19) restrictions, real-world sensor data had to be taken from the AI-HPG Archive for all testing.) The automated test (Data Flow Test #2) was divided into two parts: a single automated data run using a Clear Sky Case; and, a multi-iteration (four cycles) data flow run using Overcast Sky Case scenarios. Lessons learned from these tests are captured in Section 5, followed by a return to the Future Vision, and Results and Conclusions.

The purpose of this study was to prove (or disprove) that in-situ-only atmospheric intelligence could automatically be acquired, processed, and converted into actionable information employed by an automated power conversion, optimization, and AI-HPG Test-bed emulator applications (simulating the AI-HPG Test-bed, due to COVID restrictions). This automating goal has now been successfully proven, enabling the focus to shift onto the refinement of elements and processes that will further advance hybridized power optimization. Between the AI-HPG Feasibility Study[1] and the recent Data Flow Tests (this report), the revelation of element and system advances waiting to be pursued has constructively planted the opportunity for empowering the future Soldier and disaster relief resources.

[1] Vaucher G, D'Arcy S, Berman M. In-situ atmospheric intelligence for hybrid power grids: Volume 1 (feasibility study). White Sands Missile Range (NM): CCDC Army Research Laboratory (US); 2019 Dec. Report No.: ARL-TR-8864.

1. Introduction

The future battlefield will be filled with multiple dissimilar energy networks including unmanned and manned vehicular platforms actively engaged in cooperative control and communications capable of overpowering an adversary and dominating the battlespace. This chaotic multi-domain operational environment will be limited by variable operating conditions (mission profiles, terrain, atmospheric conditions), copious amounts of real-time actionable intelligence derived from weapon and sensor suites, and most importantly, the energy capabilities of each platform.

To achieve dominance within the battlespace, energy flow characterizations of individual platforms and the aggregate battlespace must be developed with respect to the variable operating conditions. As an example, consider the power-requirement differences between the General Atomics MQ-1 Predator (an unmanned aerial vehicle), the Gladiator Tactical Unmanned Ground Vehicle, and the Mine Countermeasures Unmanned Surface Vessel (an unmanned sea vehicle). The predator is designed to provide air superiority, support fires, maneuvers, communication, and coordination-based missions. The Gladiator supports fires, maneuvers, communication, and coordination-based missions. The mine countermeasures vessel is designed to assist with maneuver and coordination-based missions and could be extended to support fire-based missions. Current and future military operations will routinely coordinate with multiple dissimilar heterogeneous systems spanning multiple domains resulting in Multi-Domain Operations (MDO).

While the operational domains may vary, each is limited in its capabilities by energy dissipation, storage, and generation requirements. Other critical factors include meteorological/hydrological conditions and the imposed mission profile. Each military vehicle represents a collection of self-contained energy flow networks containing producers, suppliers, and energy storage devices. The aggregation of these networks results in a mobile energy network or microgrid. Such systems also support the ability to interconnect with either stationary energy networks such as a Combat Outpost (COP) and Forward Operating Base (FOB), or temporary ad hoc energy networks, such as vehicle-centric microgrid. In both cases, energy resources may be shared and used to exploit various mission packages that extend the capabilities of the Warfighter. The complex interdisciplinary interactions between the dissimilar energy flows are further complicated by the variable operating conditions, such as system efficiency and mission effectiveness, which may be significantly reduced, inhibiting the ability of the Warfighter to maintain current operations. In an effort to minimize system inefficiencies and

maintain adequate mission effectiveness, the development of optimal and efficient energy management and control is a key contributor. For energy management that is dependent on atmospheric resources, acquiring and exploiting local atmospheric intelligence is a fruitful strategy.

Consider an energy network that is commissioned to operate for the next 48 h. Let this network consist of a 30-kW diesel generator, 10-kW photovoltaic (PV) array (subject to a clear sky), 360-kWh battery storage (at a 24-h discharge rate), and a variable electrical load. Let the variable load be composed of two load types: one which is invariant of the operating environment and one which is a function of atmospheric conditions (such as the load to run heating, ventilation, and air conditioning [HVAC] units). Electrical load, atmospheric conditions, and generator fuel consumption characteristics examples are provided in Figs. 1, 2, and 3, respectively. For this example, the resulting electrical load requires 700 MJ of energy. This energy must be provided by the generator, storage, PV array, or some combination of the three. Assuming there is no future atmospheric intelligence, the PV array will likely be underutilized and as a result, excess fuel and energy storage requirements will likely be incurred.

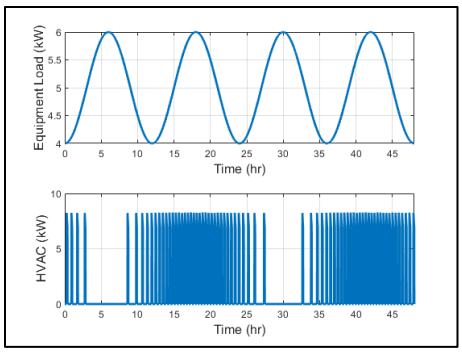

Fig. 1 Example microgrid electrical load profile

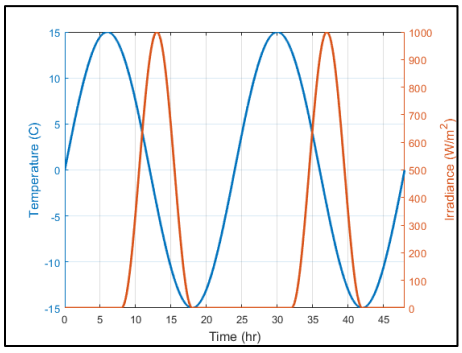

Fig. 2 Example atmospheric conditions

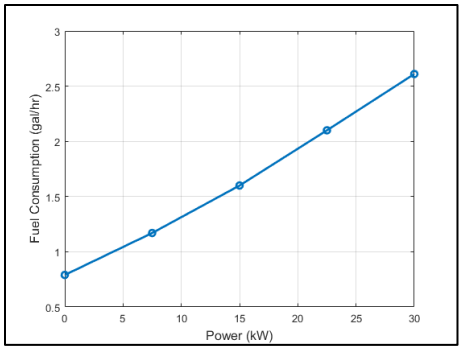

Fig. 3 Example fuel consumption characteristics

With no atmospheric knowledge, one feasible operational solution would be to run the diesel generator continuously, servicing the entire electrical load. Any and all energy storage generated by the PV would, by default, be stored within the energy storage as a result of the sky conditions. The results of which are shown in Figs. 4–6.

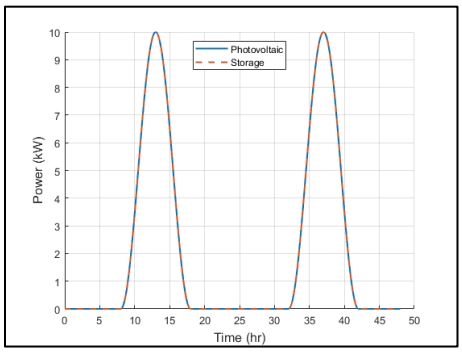

Fig. 4 No atmospheric knowledge case results: PV and energy storage power requirements. (The sign of the PV and storage power are opposite; positive indicates that the PV array is supplying power, while positive storage power indicates that the storage is charging. Similarly, negative storage power indicates that the storage is discharging.)

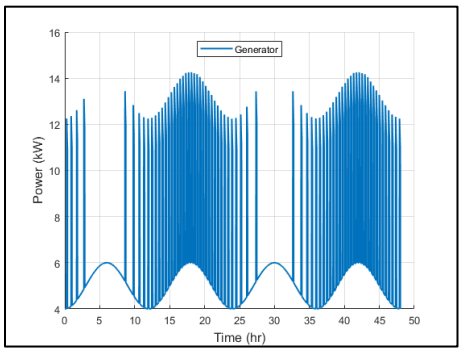

Fig. 5 No atmospheric knowledge case results: diesel generator power requirements

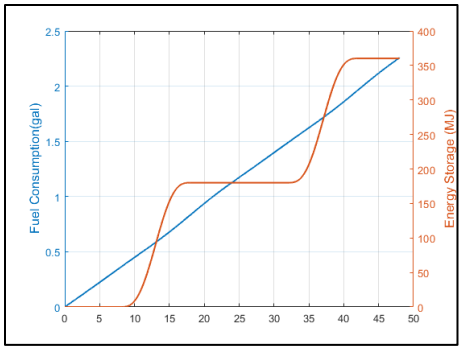

Fig. 6 No atmospheric knowledge case results: fuel consumption and energy storage performance metrics

For this solution, the energy storage must have a minimum storage capacity of 360 MJ and must have sufficient space to store the generated energy. Further, the diesel generator will consume 2.35 gal of diesel fuel. However, this is not a good use of the PV. A more optimal use of the PV (assuming no future atmospheric knowledge) would be to analyze the PV contribution obtained for the first 24 h. This energy resource results in 180 MJ. Using this knowledge, it is fair to assume that the energy storage will continuously discharge at a constant rate for remainder of the 48-h period, and discharge 180 MJ, while the remainder of the electrical load is then serviced by the diesel generator. The results of this strategy are provided in Figs. 7–9.

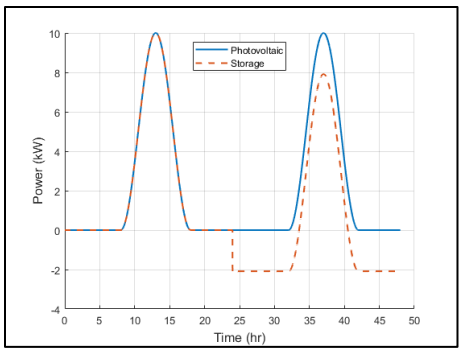

Fig. 7 Current atmospheric knowledge case results: PV and energy storage power requirements. (PV and storage power signs are opposite; positive indicates that the PV array is supplying power, while positive storage power indicates that the storage is charging. Similarly, negative storage power indicates that the storage is discharging.)

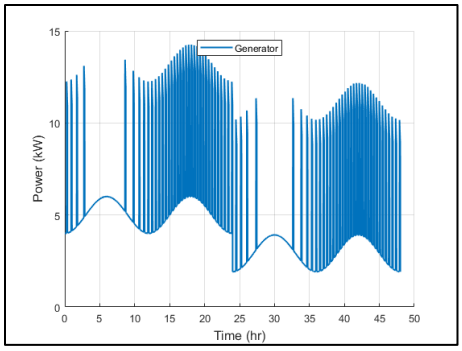

Fig. 8 Current atmospheric knowledge case results: diesel generator power requirements

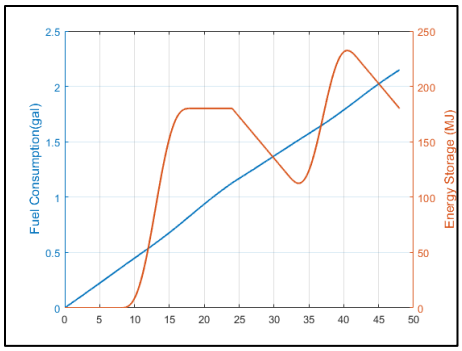

Fig. 9 Current atmospheric knowledge case results: fuel consumption and energy storage performance metrics

In contrast, by incorporating minimal atmospheric intelligence observed from the previous days' performance metrics, the minimum storage capacity can be reduced to 225 MJ, and the diesel generator fuel consumption can be reduced by 4.4%, consuming 2.15 gal of diesel fuel. This solution is more optimal in regard to both fuel and energy storage requirements; however, this may not always be the case. Diesel generators operate closer to their peak efficiency at higher loads and the fuel inflection points tend to be near half the rated power capabilities. As a result, when the load is reduced on a generator, less efficient operation is expected. Reduced efficiency can lead to increased fuel consumption for extended operational periods.

If future atmospheric intelligence were available and combined with the fuel consumption characteristics of the diesel generator, a more optimal energy management solution could be theorized. The atmospheric intelligence most relevant to this hybridized microgrid example would be the PV-dependent variables, such as solar radiation and panel temperatures. With these attributes, the resulting PV energy generation capabilities can be calculated and the electrical load estimated. Assuming the future atmospheric intelligence was available, one could 1) generate a more optimal fuel solution to run the diesel generator at its rated capacity, 2) charge the energy storage, and 3) accommodate the electrical load.

In the 48-h mission example, for the first hour, the diesel generator was used to service the aggregate electrical load and charge the energy storage. For the next 19 h, the electrical load was serviced by the energy storage and the PV array. At hour 20, the diesel generator was brought back online for the next 4 h at 16.5 kW (little over half the rated generation capacity) to charge the energy storage and service the electrical loads, in combination with the energy storage. For the remainder of the 48-h period, the generator remained off and all power required to service the electrical load was provided by the PV array and the energy storage. The results of this example are provided in Figs. 10–12.

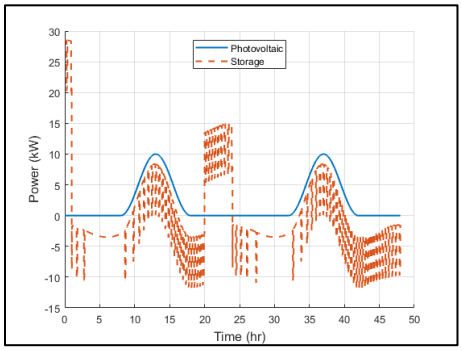

Fig. 10 Current and future atmospheric knowledge case results: PV and energy storage power requirements. (The sign of the PV and storage power are opposite; positive indicates that the PV array is supplying power, while positive storage power indicates that the storage is charging. Similarly, negative storage power indicates that the storage is discharging.)

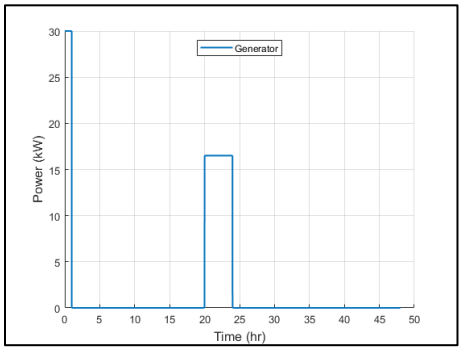

Fig. 11 Current and future atmospheric knowledge case results: diesel generator power requirements

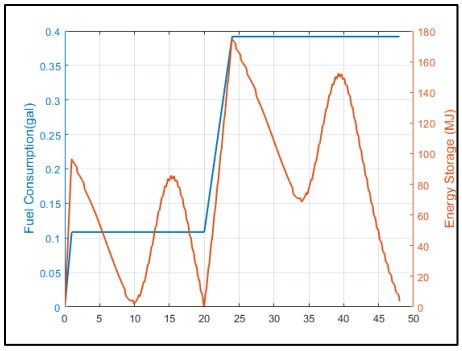

Fig. 12 Current and future atmospheric knowledge case results: fuel consumption and energy storage performance metrics

By incorporating future atmospheric intelligence into the microgrid operational intelligence (describing current and future microgrid behavior), the minimum storage capacity could be reduced to 180 MJ and fuel consumption of the diesel generator could be reduced by 81%, consuming a net 0.4 gal of diesel fuel. Keep in mind that an optimal energy solution for any energy network containing generators and energy storage will save fuel at the expense of using more energy storage; the inverse is also true. This implies that mission effectiveness and mission efficiency can be managed through energy storage and fuel consumption, based on the variable operating conditions.

The previous example demonstrates how the integration of atmospheric intelligence into the energy management system can significantly improve tactical energy generation and distribution. It follows then, to fully characterize the dissimilar energy flows and affect mission effectiveness and mission efficiency, atmospheric knowledge must be investigated and integrated within current and future power grid control strategies. By exploiting this resource, operational intelligence can better aid battlefield commanders in making informed decisions.

2. System Design

The tactical power grid design being investigated and documented looks to the future when a diversity of power resources has become “the norm”, and the performance of these integrated resources flawlessly provides uninterrupted electrical power for a multitude of platforms. This study is one of several steps intended to bridge the gap between contemporary and future power distribution optimization strategies. A summary of the long- and short-term goals follows.

While the selected design is geared for tactical applications, this research is equally applicable to designing and operating mobile emergency power resources that might be deployed immediately after a natural disaster.

2.1 Long-Term Vision

Ensuring battlefield overmatch under all phases of MDO requires significant tactical and strategic awareness of assets, their states, and their capabilities. Energy availability is a key element of those assets. This project seeks to develop and demonstrate the ability to utilize organically obtained atmospheric knowledge to forecast and optimize a hybridized grid's short-term energy needs and availability. The current effort focuses on effectively integrating PV as a source of local energy for demonstrative purposes. However, the longer-term goal includes a wide range of locally sourced energy including hydroelectric, wind, geothermal, as well as foraged energy sources.

2.2 Short-Term Vision

This research study has evolved in phases. In Phase I, a not-yet-constructed hybridized tactical power grid was simulated. One of the key results from that exercise was documenting a quantified fuel reduction when atmospheric intelligence was introduced to the grid-optimizing routine. In Phase II, the modeling of key atmospheric variables was introduced, and a requirement that all contributing resources would need to be locally derived was imposed. This latter restriction provided the novel framework for the study's tactical and disaster relief applications. Phase II also raised the question regarding whether the simulation work could be proven in a real-world setting.

Phase III answered the lingering question, and was executed under the Atmospheric Intelligence for Hybrid Power Grid (AI-HPG) Project. This parallel project focused on investigating the construction of an AI-HPG Test-bed that would 1) generate data that could prove/disprove the feasibility of the integrated, simulated hybrid power and 2) provide additional real world measurements useful to future simulation work. Coincident with Phase III was a proposed employment of artificial intelligence (AI) and machine learning (ML) research techniques, and their need for significantly larger data resources. Constructing an AI-HPG Test-bed expanded its goals to include becoming just such a real-world data resource, if automated.

In ARL-TR-8864 (Vaucher et al. 2019), the feasibility and design of the AI-HPG Test-bed was documented. Several lessons learned were considered, including the next step—to automate the AI-HPG Test-bed process. The following sections document the success of this subsequent step and define future goals gleaned from the Data Flow Test #2 experiences.

3. System Elements

The AI-HPG Test-bed design consists of three major components: the atmospheric intelligence, the power optimization, and the acquisition of data for the purpose of improving the previous components. Sub-steps for these major components are outlined as follows:

1. Atmospheric Intelligence Component
    1.1 Panel Temperature Acquisition
    1.2 Solar Radiation Calculation
        1.2.1 Whole Sky Imager Image Acquisition
        1.2.2 Whole Sky Imager Image Analysis
        1.2.3 Solar radiation model to calculate current/future solar radiation
2. Power Optimization Component
    2.1 Power Conversion
    2.2 Power Optimization
    2.3 Integrate optimization solution into an emulated AI-HPG Test-bed
3. Data For Model Improvements Component
    3.1 Pyranometer data acquired to improve solar radiation methods
    3.2 Power train data acquired to improve optimization routines

A description of the overall system and each system element follows.

3.1 Hardware

The hardware used in this project (see Fig. 13) included a collection of environmental sensors (thermometer, Whole Sky Imager [WSI], pyranometer), plus the original AI-HPG Test-bed with solar power, battery storage, programmable load, and a data acquisition system to record power measurements for each component. The function of each element was either to record real-world operational data or to be used as a calibration of the model and simulation results.

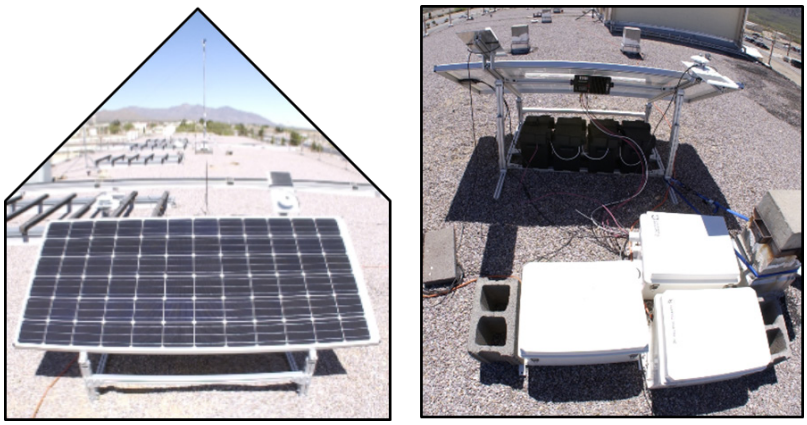

Fig. 13 Original AI-HPG Test-bed showing the design. Miniature WSI (not shown here) replaced the original simulated-WSI Camera System in 2020. (Vaucher et al. 2017)

The environmental sensors that provided operational data included the WSI and the Panel Temperature probe. The WSI used a Raspberry Pi camera with a fisheye lens to produce an image of a full hemispherical sky field of view. The panel temperature was measured by a DS18B20 temperature probe attached to the back of the solar panel. Unlike the ambient temperature measurements, there was no requirement to aspirate the probe. Consequently, temperatures were generally warmer during the day than the National Weather Service temperatures and represented only the thermal characteristics of the PV panel.

The solar irradiance measurements were taken by a Kipp and Zonen CM3 pyranometer attached to a Campbell data logger. These samples were acquired to calibrate the solar radiation values calculated during the automated AI-HPG Data Flow Tests.

The power train measurements were recorded as current and voltages for the PV, battery, and load. These data served as post-test power validation resources. The solar power consisted of a 325-W PV panel feeding a Midnite Solar maximum power point tracker (MPPT) charge controller, powering a set of three 8-V sealed lead-acid batteries in series, with approximately 160 Ah of capacity. The load was generated by a BK Precision 8510 digital load, and the voltage and current measurements were collected by a National Instruments CompactDAQ data acquisition system. The load was programmable, an attribute that was a key component for observing the grid optimization command effects.

3.2 Automating Script

Automating the data collection, analysis, optimization, and execution processes was a critical milestone of this Phase III research. Creating a modular strategy was a vital attribute to ensure the accommodation of future technical advancements. To

that end, an overarching structure was developed to weave the individual components into an integrated system.

A MATLAB object was created to manage program flow and the associated data. The primary methods of this object corresponded to each phase of the data analysis and forecasting as well as the loop implementation. Several ancillary housekeeping methods were also included. Figure 14 illustrates the structure of the executive object. The primary methods to execute the analyses began with “get”. A new or modified analytical method was easily implemented creating a new child object that overrode the desired “get” method with the new behavior.

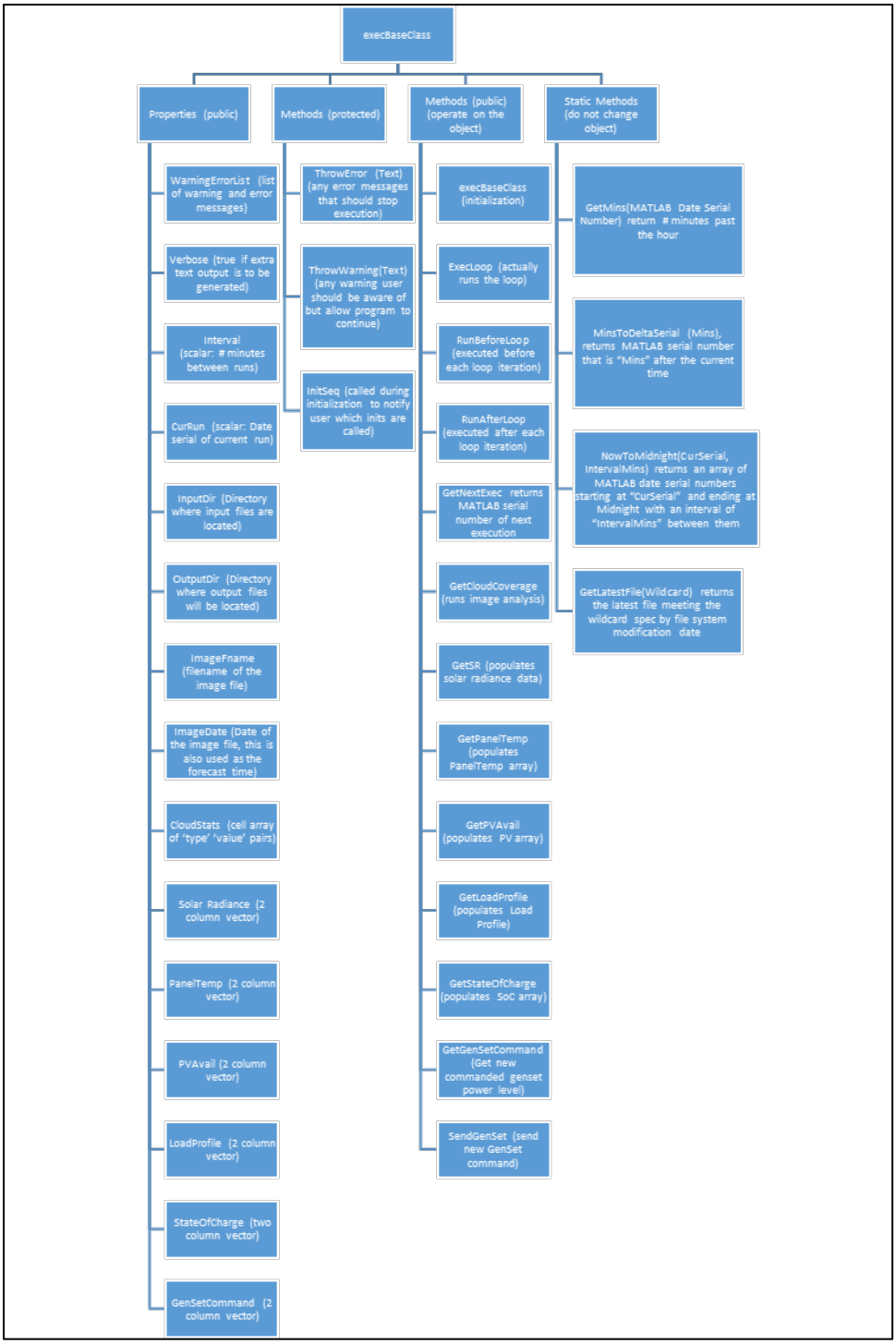

Fig. 14 Executive object structure

There were three other main methods implemented by this object. The "ExecLoop" method initiated and managed the main program loop that ran continuously and periodically called each of the "get" functions in the appropriate order. The "RunAfterLoop" and "RunBeforeLoop" methods were each executed once per loop

just after loop initiation and just before loop exit. These functions were used to write out diagnostic and status information as well as to initialize and clean up necessary processes. The executive object also included methods for reporting errors and warnings that maintained program synchronization and logging.

For Data Flow Test #2, the loop executed infinitely. The loop method was structured such that it was easy to implement functionality that would respond to MATLAB's event-driven architecture. Figure 15 illustrates the program flow of the main loop.

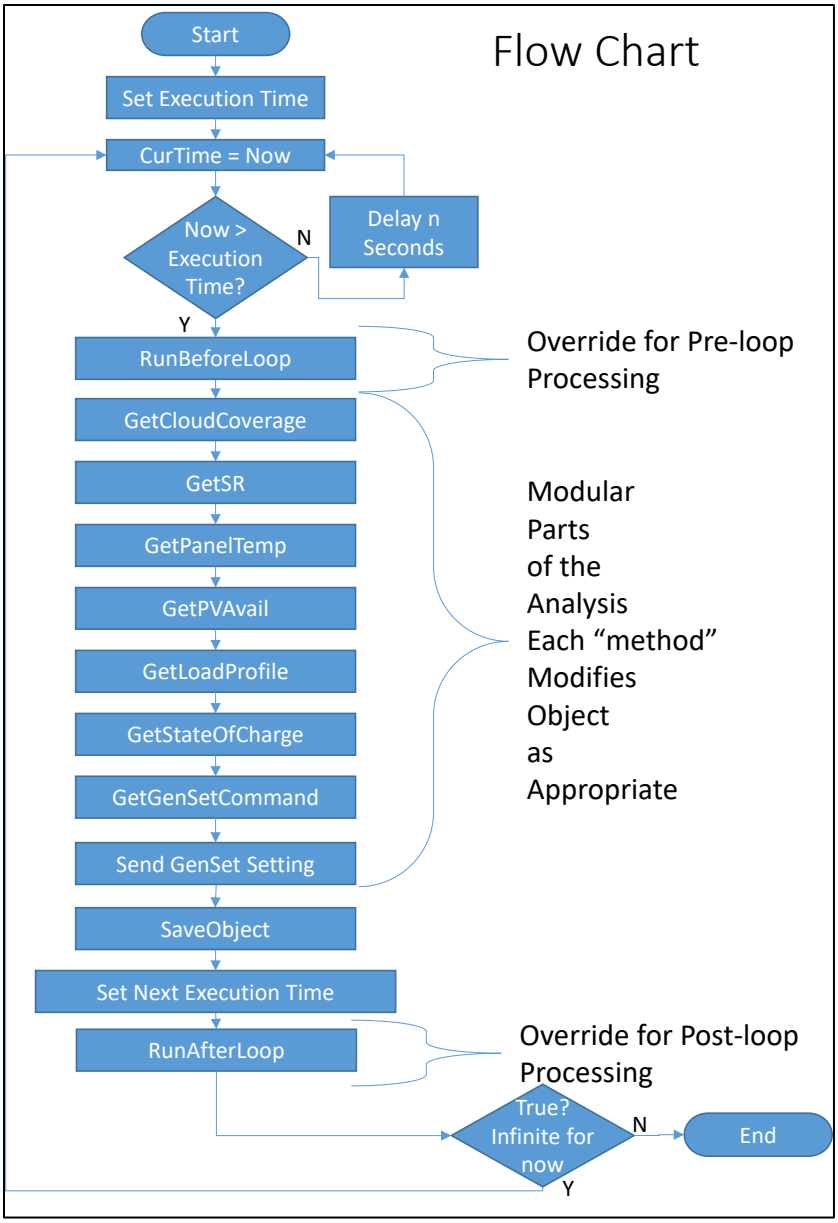

Fig. 15 Execute object loop flow

In the Data Flow Test #2 implementation, all of the data that were used as input to the "get" functions were written as ASCII files at the conclusion of the loop. The time for each iteration was synchronized with the WSI image time, regardless of the current wall-clock time. In addition, the entire object was written out in MATLAB format, with a tag indicating the current date and time.

The structure of this executive object enabled a user to replace various elements of the analytical algorithms without affecting other elements. In addition, each element clearly defined its requirements, and the data ingress and egress were managed by the executive object, allowing the user's focus to remain on processing the data and not file input/output.

3.3 Sensor Data

The AI-HPG Test-bed collected a variety of data to support both the optimization routines and analysis of system performance (component improvement). A description of the data elements follows.

3.3.1 Panel Temperature

The first acquired element of the AI-HPG System was the PV panel temperature. This sensor was a DS18B20 temperature probe, which sent data to the Raspberry Pi system. (The Raspberry Pi also operated the WSI.) The panel temperature data were automatically sampled and recorded at 1-min intervals throughout the day. The data were provided in a file that contained a local time stamp and temperature measurements for that day. For the Data Flow Test #2, panel temperature data began at 0500 Mountain Time (MT) (sunrise twilight) and ended at 2100 MT (sunset twilight). Due to COVID-19 restrictions, the real-world data used for the Data Flow Test were extracted from the real-world AI-HPG Archive. The files used in the Test cropped the data per the date/time being represented. For example, for the 2019 September 19, 1245 Local Time (LT) run, the panel temperature file included samples for 2019 September 19, 0500 MT–1245 LT only. For a 15-min data flow cycle, the next range of panel temperatures provided to the automated system was from 2019 September 19, 0500 LT–1300 LT only.

3.3.2 WSI

The second AI-HPG System element was acquired by a WSI. The AI-HPG's WSI recorded 5-megapixel Portable Network Graphics (PNG) images of the sky, at 15 min intervals throughout the daylight hours; from 0500 to 2100 LT. These horizon-to-horizon (azimuth of 360°) images were provided to another component of the system for analysis. Due to COVID-19 restrictions, the real-world data used

for the Test were extracted from the AI-HPG Archive, representing the same day/time as the panel temperature data.

3.3.3 Validation Data

Two datasets were acquired to help improve the two major automated AI-HPG components. To advance the solar radiation calculations, pyranometer data were acquired. To advance the optimization routines, data were sampled at three spots in the power train. These will each be described in Sections 3.3.3.1 and 3.3.3.2.

3.3.3.1 Solar Radiation

Two research-grade pyranometers mounted on the top of the PV panel provided measured, in-situ solar radiation measurements for the AI-HPG Test-bed location. Due to sensor overhead (cost and logistics), these data were not intended to be part of the long-term AI-HPG data flow process, but rather were intended to be an independent calibrating 'truth' for the atmospheric intelligence portion of the system. For additional details and examples of these data resources, see ARL-TR-8864 (Vaucher et al. 2019).

3.3.3.2 Power Data

As a tool for assessing the optimization routines, the power train data included voltage and current measurements for the PV panel, battery system, and load. In addition, a battery state of charge (SoC) was maintained, based on the power flowing in/out of the battery. These data were recorded at 30-s intervals and stored with time stamps in a daily file.

3.4 Whole Sky Image Analyses

The AI-HPG solar radiation calculation was defined using a Solar Radiation Flux model originally developed by Ralph Shapiro (Shapiro 1982) and adapted by a project member for the hybridized power application. While the 2019 AI-HPG Feasibility Study (Vaucher et al. 2019) used a graphical user interface (GUI) to execute the model (Walker and Vaucher 2017) that quantified the sky conditions, in this study, an ML model was developed to autonomously quantitate the sky conditions from a whole sky image. The key features determined by the ML model were the fractions of various cloud types observed in a given WSI image. Early attempts at automated cloud detection for satellite imagery involved hand-craft textures and features (Lee et al. 1990). With recent developments in ML-like Convolutional Neural Networks (CNNs), the computer can now learn its own feature detectors at different length scales to classify and locate cloud types in a sky image.

The AI-HPG CNN model consisted of several layers of convolution and down-sampling leading to a dense layer that predicted seven classes: cirrus, cirrostratus, stratus, stratocumulus, cumulus, blue sky, and other. The inputs to the model were blocks of 32 × 32 pixels extracted from a larger whole sky image. In this way, detected cloud types in small blocks could be "painted" onto a larger composite image. The other class ensured that objects besides clouds and sky were not included in the fractional cloud coverage calculation. In addition, a separate sun location model based on bright pixels was used to prevent the sun from being counted. It involved searching for a bright spatial Gaussian distribution of pixels in the full input image. The predicted sun brightness from this model was also used to determine whether to alleviate the effects of solar bleaching through a simple image contrast function: $(x) = x^2$.

For training, a relatively small dataset of labeled cloud images from various resources was developed. The training data count was bolstered by the fact that each training image was divided into several 32 × 32 blocks. For blue sky images, a series of blue images with variations in color saturation and value (brightness) was created.

As can be seen in Fig. 16b, the trained ML model was able to do a reasonable job on a partly cloudy image (Fig. 16a). The predicted fractions of cloud types were cirrus: 2%, cumulus: 32%, and sky: 66%. However, the ML model's performance (Fig. 16d) on a clear sky image (Fig. 16c) was poorer (cirrus: 35%, cumulus: 25%, sky: 40%), owing to the bleaching effect of the sun on the camera enclosure covering.

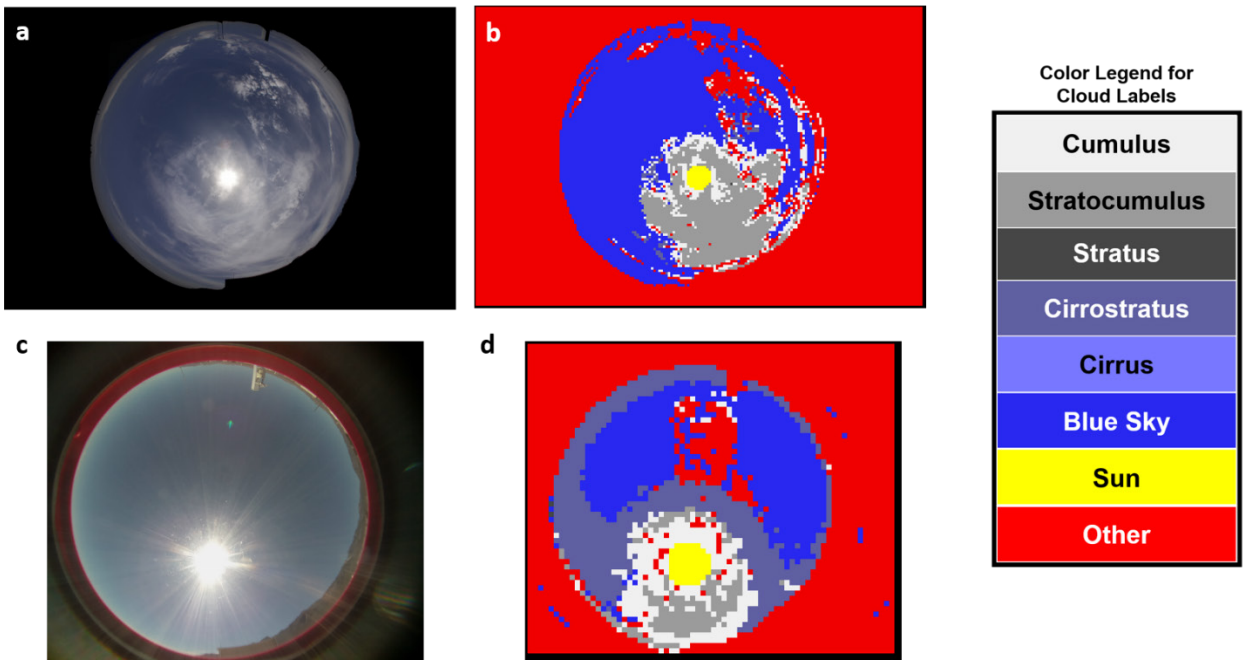

Fig. 16 a) Original partly cloudy WSI image; b) ML predictions on a); c) original clear sky image; and d) ML predictions on c)

These early results of the whole sky analysis algorithm were encouraging. Advances through clear sky corrections and/or glare-reducing improvements to the camera enclosure are being pursued.

3.5 Solar Radiation Model

The Solar Radiation model served to calculate the surface solar radiation magnitudes based on the local sky conditions. The in-situ restrictions of the system design significantly pruned the Solar Radiation model choices. In ARL-TR-8582 (Vaucher and Welch 2018), a summary of surveyed models is presented, along with the method used to identify the current best fit AI-HPG solar radiation model that satisfies both the tactical energy unit independence requirements and the practical data application.

The Solar Radiation model chosen for the AI-HPG Test-bed was based on Ralph Shapiro's Solar Radiation Flux Model (Shapiro 1982). While there are numerous factors that impact the surface solar radiation magnitudes, the model simplified these variables and implemented them in an algorithm that predicts the net solar radiation flux received at ground level throughout the entire solar day. There are two major elements in the model: 1) solar position, which is a function of the Julian date, declination angle, hour angle, and solar zenith angle and 2) the net transmission of solar radiation from the atmosphere's top down to the surface.

Starting at the atmosphere's top, the sun's incoming solar radiation is propagated downward through three homogeneous layers. The three key effects calculated include reflectance, transmittance, and absorption, which are a function of the local cloud type, thickness, and current atmospheric conditions. Weighting functions quantify the impact of the various sky characteristics (Shapiro 1982; Walker and Vaucher 2017).

When automating the model within the AI-HPG Test-bed, the cloud characterization input was further simplified to three generic cloud types and quantified in base-10 percentages. The presumption made was that the input generated from ML techniques would bridge the details lost in this smoothed input.

As with the original model's GUI, the output included a 24-h solar radiation plot and listing of the solar radiation magnitude for a user-selected time. Added to the original model were two output files: a generically labeled file included the year, month, day, and a 24-h time series for solar radiation at the surface and atmospheric top. This file was duplicated and labeled for the AI-HPG Archive. The generic file name was chosen so it could easily be overwritten in the next AI-HPG data processing step.

As an added feature gleaned from the Data Flow Test #2, the model was designed as a function so that the output could be available as a variable within the automating script. This strategy was intended to reduce system file input/output time requirements.

Figure 17 shows sample input and output from the Data Flow Test #2.

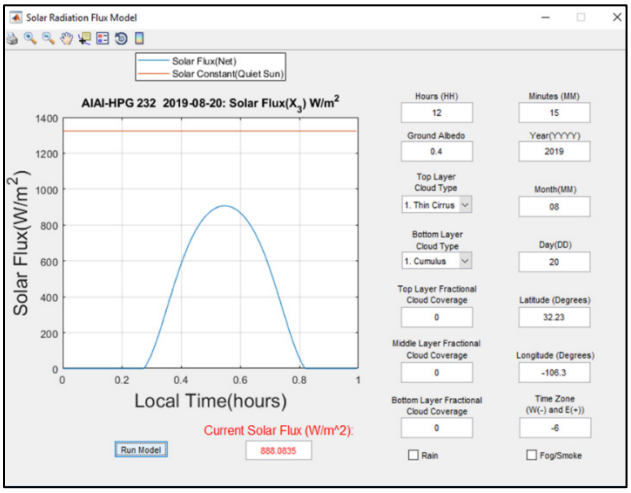

Fig. 17 Graphical user interface for the Solar Radiation Flux model input with graphed output

3.6 Power Conversion

Based on the previous AI-HPG Feasibility Study results (Vaucher et al. 2019), the Mahmoud, Xiao, and Zeineldin (M-X-Z) model (Mahmoud 2012) was utilized to predict the electrical power, given a certain in-situ solar radiation value. This module used the incident solar radiation, panel temperature, and panel model-specific vendor specified parameters to model the current-voltage (IV) curve of the panel. From that IV curve, the maximum power point was utilized to estimate the resulting power provided by the PV panel.

The previous algorithms in the automated AI-HPG sequence generate a solar radiance forecast at a specified time interval (currently 1 min), which is used as one of the primary power conversion inputs. The forecast algorithms do not predict panel temperature, which is the other primary input. The algorithm does have access to the measured panel temperature, up to the current time. For the remainder of the day the panel temperature is presumed to be the same as the previous day's temperature for that time. In the current implementation, this resulted in a discontinuity in the temperature data at the time of prediction. In future versions, this discontinuity will be smoothed by an averaging algorithm until a better temperature model is implemented.

3.7 Power Optimization

The power optimization is described in three parts: the integration of the optimization function, the function's input, and the optimization routine.

3.7.1 Integrating the AI-HPG Optimization Function

For the AI-HPG Data Flow Test #2, the optimization algorithm operated on a client-server basis. This configuration was driven by several factors including the availability of MATLAB licenses and the ease of source code access by Michigan Technological University (MTU) researchers. Executing the optimization algorithm as a server on a remote system located at MTU enabled the demonstration to leverage the real-time availability and expertise of the MTU collaborators.

3.7.2 AI-HPG Optimization Input

Input to the optimization algorithm included 24-h forecasts of solar radiation, temperature, and anticipated loads, as well as the current SoC of the energy storage system. The current solar radiance forecasting algorithms were limited to providing forecasted solar radiation values for the current day only. The panel temperature was limited to the measured values from the previous morning until the retrieval time of the latest sample. As a result, the optimization algorithm presumed that the

current 24-h period and the following 24-h period had identical solar radiation profiles, and that the temperature of the current day followed the same profile as the previous day.

3.7.3 Optimization Routine

The Energy Management System (EMS) computed a fuel-optimal generator command for the hybrid power grid whenever requested. The results were defined at fixed increments such as 15, 30, or 60 min. Implementing the generator command completed the feedback loop of a Model Predictive Control (MPC) strategy. This strategy required two-way communication between the supervisory controller on the AI-HPG Platform and the MTU-EMS. Classes were written in MATLAB for both the EMS and AI-HPG Platform to manage all the necessary tasks, from establishing communications through providing an optimal generator solution.

The EMS fuel-optimal solver required the following information to be passed to it from the supervisory control system:

- dt: Update period (minute, e.g., 15, 30 or 60)
- pPVNOW: the most recent measurement of PV output from the AI-HPG Test-bed (kW)
- pPVFUTURE: a 24-h forecast of PV output (kW) at the interval indicated by dt
- pLodNOW: the most recent measurement of the electrical load on the grid (kW)
- pLodFuture: a 24-h forecast of electrical grid load (kW) at the interval indicated by dt
- eSoC: the most recent measurement of energy storage state of charge (kJ)

The solver used a two-tiered approach for finding a set of generator commands that, if applied over the next 24 h, theoretically would result in minimum fuel consumption. The EMS then sent to the supervisor only the generator value that should be used for the next dt minutes, while the remaining generator settings were discarded. The first stage of the solution process used a Genetic Algorithm (GA) to develop a feasible generator command set. The second stage used the GA's solution as the initial guess to a gradient-based numerical optimization routine that refined the solution. For a dt = 15 min scenario, the number of generator commands that were computed was 96 and took about 30 s to solve—well within the dt =15 solution period.

A key assumption in this solution approach was that the generator efficiency curve was known. Typically, diesel generators consume more fuel per kilowatt when operating at low power output. Therefore, the EMS solver typically drives the generator to operate at a high power output. For the recent tests, a generator was emulated that had a peak output of 0.1 kW, with peak efficiency occurring above 0.05 kW. The small generator size was established commensurate with the PV output available in the AI-HPG Test-bed. A typical generator solution (blue) is shown in Fig. 18 where the electrical load was held constant at 0.104 kW (black) with the measured PV (green). The generator solution shows the expected on/off behavior and always operates in the maximum efficiency regime.

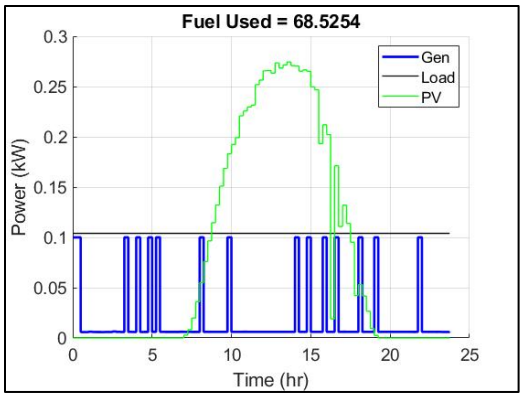

Fig. 18 Typical 24-h, fuel-optimal generator solution provided by the EMS in response to inputs from the supervisory controller running on the AI-HPG Platform

The EMS fuel-optimal generator solver constrained the grid's battery system SoC to return to its starting value every 24 h. The initial SoC value was automatically latched the first time a solution was requested or was reset by the supervisory controller running on the AI-HPG Platform. This introduced a potentially useful feature for future study, where the 24-h target SoC can be modified by an intelligent agent running on the supervisor. For example, the SoC constraint could be relaxed during times of critical, extreme power requirements, and then brought back to a safe level later.

The generator solution was further constrained to ensure the maximum energy storage capacity was not violated. This was important from a practical perspective, but also aided in determining storage and PV requirements for hybrid grids. For example, given maximum load scenarios and irradiance information, the storage capacity and PV could be iterated to demonstrate their optimal values. This attribute has the potential for reducing weight, volume, cost, or other metrics when designing a deployable system.

3.8 AI-HPG Test-bed Emulator

Implementing the optimization solution on the real-world AI-HPG Test-bed was inhibited by COVID-19 restrictions. Consequently, an indirect demonstration of implementing the solution was created by developing an AI-HPG Test-bed Emulator. This LabVIEW emulator device was designed to

- read the observed solar power data and optimization output (when available),
- calculate the generator load and battery power data,
- determine the battery's SoC, and
- output all (PV, battery, load) power data and a new SoC.

While operating, the AI-HPG Test-bed Emulator calculated the SoC status for each line of PV data (recorded at 30-s intervals). The process included ingesting the current load profile, initial SoC,[*] actual PV power (from the previously measured AI-HPG Test-bed source), and the latest optimization solution (*newgensetval.txt*).

These data, plus the SoC calculated for the previous step, were processed and a new SoC was generated. Researchers could observe this SoC via the Net Battery Power graphic on the Test-bed emulator. The data processing included calculating the net power input/output, and integrating over the given time interval (30 times over a 15-min interval).

The load profile had a preprogrammed step function that changed, independent of atmospheric conditions. This attribute served to challenge the optimization routine. The load changed at the time of a new iteration (15-min intervals).

Using the AI-HPG Test-bed Emulator, the final step of the process produced an output that consisted of power data (actual PV, battery, and load were calculated), and a new SoC. These output data were generated to help calibrate and refine future optimization strategies.

4. Data Flow Tests

Two Data Flow Tests were conducted in 2020. The first was in June 2020 and the second in July 2020. A brief summary of each event follows. For additional information, see Appendixes A and B.

[*] Initial SOC means the SOC used for Step 1.

4.1 Data Flow Test #1

The first AI-HPG Data Flow Test was conducted on 2020 June 3. Three pretests were executed to pre-evaluate the AI-HPG data flow elements. Subdividing the process into two major parts (Atmospheric Intelligence and Power Optimization), the following order of elements was tested:

Atmospheric Intelligence:

- Sensor Data – Panel Temperature
- Sensor Data – WSI Images
- WSI Analyses
- Solar Radiation Modeling

Power Optimization:

- Power Conversion
- Power Optimization
- Power Validation

The platform used to execute the data flow test was a Linux PC. Test execution was conducted via remote access, due to COVID-19 telework requirements and participants being in five unique locations; some were separated by over 1400 miles. The Linux PC activity was viewed by all participants via Microsoft Teams. An independent parallel data flow execution was concurrently conducted, proving multiuser capabilities and validating iterative results. For details concerning the major steps of the data flow process, see Appendix A.

4.2 Data Flow Test #2

The AI-HPG Data Flow Test #2 was subdivided into two parts: a single Clear Sky Case, and a sequence of multiple Overcast Cases. The data flow was predefined as follows:

1. Acquire measured data (Panel T, WSI).
2. Calculate current and future solar radiation for a 24-h period.
3. Convert measured and forecasted atmospheric values into PV power generation.
4. Generate an optimal power grid solution.

5. Implement that optimal solution and sample the actual current/voltages for PV, battery, and Load to determine the true power generated for the given time interval.

The predefined start-run time interval was 15 min for the sampled data, based on earlier studies (Jane et al. 2020). Due to the use of archived data separated by 15 min, the automating routine advanced the cycle after a 4-min actual time period. Images were manually updated into the cue.

For details concerning the Data Flow Test #2 data flow process, see Appendix B.

5. Lessons Learned (by Element)

Following each Data Flow Test, an Internal Project Review (IPR) was conducted. Four questions were asked regarding what went right, what needs to be improved, a future vision for each element, and any comments. A summary of the feedback provided during these IPR follows.

5.1 Hardware

The AI-HPG Test-bed hardware used to generate the archived data files continues to function without human intervention, with data being preserved on an independent data acquisition platform. Reviewing the processed input data, it was noted that the hardware for weatherproofing the WSI has potential for a self-imposed glare that needs to be addressed. Improved cleaning and maintenance for a new WSI dome is currently being pursued. Post-COVID plans include integrating live real-world data into the automated AI-HPG process.

5.2 Automating Script

The Executive Script/object needs to include methods for reporting errors and warnings, and to define appropriate responses to such events. Ensuring the mix of algorithmic elements compiled with the executive object's error reporting mechanisms will better enable capturing and quickly responding to system behavior anomalies, in the context of the total data flow goals.

The collage of elements is currently centered around a MATLAB resource for computer coding. Converting the code into another less costly, mathematically capable platform, such as Python, could be a more fruitful and fluid alternative.

5.3 Sensor Data

The panel temperature sensor values currently read in text form. Consequently, extra care needs to be taken to avoid ingesting extraneous characters.

The governing Raspberry Pi (data processor) requires the addition of a real-time clock to avoid time stamp errors, as the network-based clock can go backward under intermittent network connectivity.

The WSI auto-exposure routines tend to work poorly when the sun is in field of view. Special measures, based on the original simulation-WSI (professional camera) experiences need to be pursued to prevent over-exposed images under most sky conditions.

5.4 Validation Data

Solar radiation data acquired by the research-grade pyranometers continues to sample data without human intervention. As the solar radiation calculation advances, these data files will become more critical for calibrating improvements.

The AI-HPG System does a reasonable job of estimating the effect of power conditions on the SoC. However, measured power losses due to the actual battery charge/discharge, may have limited value, since individual battery types produce distinct power losses. In particular, the charging losses of a lead acid battery change dramatically with changes in the battery SoC. This pattern is much less pronounced in newer battery technologies, such as lithium-ion.

5.5 Whole Sky Image Analyses

Early results of whole sky analysis algorithm were encouraging. The strategies used to analyze the images are continually evolving. As more learning data become available (through the AI-HPG Test-bed and other resources), the time between learning and improvements will shorten. More specifically, advances regarding clear sky corrections and/or glare-reducing improvements to the camera enclosure are being pursued.

5.6 Solar Radiation Model

There are several directions this model can evolve. As more in-situ data become available, the current weighted functions can be tailored for the site. A parallel independent study exploring the use of AI/ML for determining and forecasting solar radiation is reaching its first major milestone. This AI/ML approach may make a

good supplement to the adapted Solar Radiation Flux Model currently used by the AI-HPG Test-bed.

5.7 Power Conversion

One of the primary weaknesses in the power conversion algorithm is the assumption that today's panel temperature profile is identical to yesterday's profile. Until a method for accurately forecasting panel temperature is available, the forecast temperature for the current 24-h period should be a scaled variation of the previous 24-h period.

5.8 Optimization

Errors encountered by the client or server need to be reported back to the calling program, with an indication that the new optimization setting cannot be computed.

Several AI-HPG Test-bed PV profiles were used to develop load scenarios for the tests. However, the PV output used during the tests was about 40% lower than any of the development profiles. Therefore, the electrical load scenario was large relative to the amount of PV energy available. Fortunately, the EMS solver functioned properly, but just barely. Future tests should use a lower load scenario. In addition, longer runs should be undertaken using some of the feature-rich load scenarios. These changes will better illustrate the benefits of using an EMS where the storage system charges in advance of expected future electrical demand.

There are a few improvements to be made to the optimization setup. Each time the EMS computes a solution it archives its state, including the data it received and the 24-h solution it computed. While the forecasted storage SoC was computed during the optimization process, it was not saved, since it could easily be computed via post-processing. A minor improvement would be to archive the forecasted SoC during operation to avoid the post-processing calculations.

The SoC constraint was active during the tests but was set to re-initialize with each new solution call. A rolling SoC constraint should be used in the next set of tests. This attribute will be very important when running for 24 h or more.

5.9 Test-bed Emulator

The AI-HPG Test-bed Emulator was specifically designed to answer the restrictions impose by the concurrent COVID-19 situation. Fortunately, the LabVIEW Emulator is transferable to the actual AI-HPG Test-bed, once some protocol issues are resolved. This addition to the data flow process should bring some very constructive and productive opportunities to the AI-HPG project.

6. Future Vision

The future vision for the stand-alone hybridized power grids and their need for optimization strategies continues to span multiple platforms, from powering swarms of mini-bots, tactical vehicles, and communication tools to basic tactical and disaster relief community electrical power support. With this data resource and testing platform, this research is primed for extending the experiences gained into these and other applications.

7. Results and Conclusion

The purpose of this study was to prove (or disprove) that in-situ-only atmospheric intelligence could be *automatically* acquired, processed, and converted into useful information, bolstering the quest to optimize an energy-independent, tactical, hybrid power grid. This automating goal has been successfully reached, with constructive refinements defined. Between the AI-HPG Feasibility Study (Vaucher et al. 2019) and the recent Data Flow Tests, the foundation for advancing the future integrated power mission has been established, with developing fully reliable, consistent, uninterrupted electrical power resources still the guiding long-term vision.

8. References

Jane R, Parker G, Vaucher G, Berman M. Characterizing meteorological forecast impact on microgrid optimization performance and design. Energies. 2020;13:577.

Lee J, Weger RC, Sengupta SK, Welch RM. A neural network approach to cloud classification. IEEE Transactions on Geoscience and Remote Sensing. 1990;28.5:846–855.

Mahmoud Y, Xiao W, Zeineldin H. A simple approach to modeling and simulation of photovoltaic modules. IEEE Transactions on Sustainable Energy. 2012:185–186.

Shapiro R. Solar radiative flux calculations from standard surface meteorological observations. Air Force Geophysics Laboratory (MA): Air Force Systems Command; 1982 Mar. Report No.: AFGL-TR-82-0039. Chapters 3 and 5 22–24, 38–39.

Vaucher G, D'Arcy S, Berman M. In-situ atmospheric intelligence for hybrid power grids: Volume 1 (Feasibility Study). White Sands Missile Range (NM): CCDC Army Research Laboratory (US); 2019 Dec. Report No.: ARL-TR-8864.

Vaucher G, Forrester J, Curtice M, Young R, Walker C, D'Arcy S. Atmospheric renewable energy research, volume 4: atmospheric renewable energy field study #2 (ARE2). White Sands Missile Range (NM): Army Research Laboratory (US); 2017 Oct. Report No.: ARL-TR-8198.

Vaucher G, Welch A. Atmospheric renewable energy research, volume 6 (atmospheric renewable energy field study no. 3 and preparation for tactical power in-situ atmospheric intelligence). White Sands Missile Range (NM): Army Research Laboratory (US); 2018 Nov. Report No.: ARL-TR-8582.

Walker C, Vaucher G. Atmospheric renewable energy research, volume 5 (solar radiation flux model). White Sands Missile Range (NM): Army Research Laboratory (US); 2017 Sep. Report No.: ARL-TR-8155.

Appendix A. Atmospheric Intelligence for Hybrid Power Grids (AI-HPG) Data Flow Test #1: Quasi-automated Element Checks

A.1 Atmospheric Intelligence for Hybrid Power Grids (AI-HPG) Data Flow Test #1

On 2020 June 3, the Atmospheric Intelligence for Hybrid Power Grids (AI-HPG) Data Flow Test was successfully conducted, having completed three pretests, to pre-evaluate the AI-HPG data flow elements. The data flow process was subdivided into two major parts (Atmospheric Intelligence and Power Optimization); the following order of elements was tested:

Atmospheric Intelligence:

- Sensor Data – Panel Temperature
- Sensor Data – WSI Images
- WSI Analyses
- Solar Radiation (SR) Modeling

Power Optimization:

- Power Conversion
- Power Optimization
- Power Validation

A Linux PC platform was used to execute the data flow test. Test execution was conducted via remote access due to 2019 Corona Virus Infectious Disease (COVID-19) telework requirements and participants being located in five unique locations. The Linux PC activity was viewed by all participants using Microsoft Teams. An independent parallel data flow execution was concurrently conducted, proving multiuser capabilities and validating iterative results. The following summarizes the major steps of the data flow process:

STEP 1: Atmospheric Intelligence – Photovoltaic (PV) Panel Temperature (Panel-T)

Input – Panel T. Complying with COVID restrictions, real-world data were selected from the AI-HPG Archives. The study selected a Clear Sky Case sampled on 2019 September 18.

Output – Panel T. The output file consisted of an eight-column dataset for 2019 September 18, 0500–2059 Mountain Time (MT), called *1_Output_PanelT.txt*. In a subsequent Power Conversion step, this file was *AIHPG_panelT_191007_full.txt_msb*. Both files used the following format:

Station# YYYY MM DD hh mm ss T (Celsius).

STEP 2: Atmospheric Intelligence – Whole Sky Imager (WSI). One of the improved WSI Image Analysis program features was the ability to analyze both .jpg & .png formats.

Input – WSI. Complying with COVID restrictions, real-world data from the AI-HPG Archives were used. The Clear Sky Case selected was sampled on 2019 September 18, at 1200 MT; and called, 2*_Output_WSIImage.jpg*. See Fig. A-1.

Fig. A-1 Whole sky imager image used for AI-HPG Data Flow Test #1 represented a Clear Sky Case, from 2019 September 18, at 1200 MT

Output – WSI. The analysis output was captured in a screen shot (see Fig. A-2). The *3_class_labels.1.png* file was also saved for Post-Test review.

```
(tf1) bash-4.2$ python predict_clouds.v5.py ../*Test/*.jpg
================================================
File list to process: ['../200603_DataFlowTest/2_Output_WSIImage.jpg']

------------------------------------------------
Image #1: ../200603_DataFlowTest/2_Output_WSIImage.jpg
Original image dimensions:      (972, 1150, 3)
2x downsampled image dimensions: (972, 1150, 3)
# blocks to analyze:            4130
------------------------------------------------
------------------------------------------------
Fraction of image with clouds or sky = 54.3 %
------------------------------------------------
------------------------------------------------
 Cloud-type percentages
------------------------------------------------
Cumulus       = 68.5 %
Cirrus        =  6.0 %
Stratus       =  3.1 %
StratoCumulus = 20.6 %
CirroStratus  =  1.8 %
BlueSky       =  0.0 %
------------------------------------------------
 Total cloud-sky mix
------------------------------------------------
Cloud         = 100.0 %
Sky           =  0.0 %
================================================
(tf1) bash-4.2$ python predict_clouds.v5.py ../*Test/*.jpg > predict_clouds.stdout.200603
(tf1) bash-4.2$
```

Fig. A-2 Data Flow Test #1, WSI analysis output sent to the operating platform

STEP 3: Atmospheric Intelligence – Solar Radiation (SR) Model

The SR model input consisted of a series of default values describing the surface-air/ground character, and, manually entered values for date, time, and cloud amount/layer. The model's graphical user interface (GUI) included default values for the surface layer and were supplemented by sum-total percentages for cirrus, stratus, and cumulus cloud types calculated from the WSI output. With the addition of a blue sky quantity, the total sky conditions represented 100% of the sky coverage.

The automatic output file(s) consisted of a generic *SR.dat* file, which was added to the program's directory (*200603_DataFlowTest* directory). The file format was as follows:

- Line 1: YYYY MM DD
- Lines 2 to 1441: Time (min after midnight), $SR_{Surface}$, $SR_{Top\ of\ Atmosphere}$

Snapshots of the output follow (see Figs. A-3 and A-4):

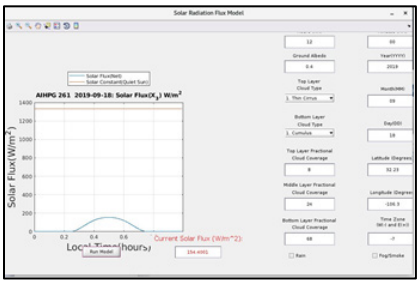

Fig. A-3 SR model GUI, showing the AI-HPG Data Flow Test #1, 2019 September 18 input and output

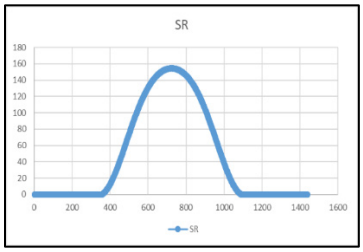

Fig. A-4 SR model data calculated for 2019 September 18

STEPS 4 AND 5: Power Conversion and Optimization

These steps were combined into a single summary due to their fluid nature.

Input. Input consisted of Panel T data from 2019 September 18. The SR data calculated from the concurrent WSI image acquired were graphically previewed and found to be acceptable.

Output. Output for the 2019 September 18 case included panel power and pGen, which were graphically reviewed (see Fig. A-5).

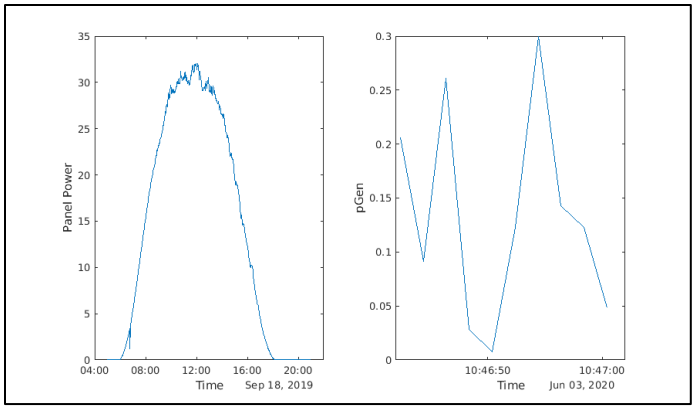

Fig. A-5 2019 September 18 Panel Power and pGen output data from the AI-HPG Data Flow Test #1 conducted on 2020 June 03

STEP 6: Power Train

The measured power coming from the AI-HPG Test-bed PV panel, battery, and load were retrieved from the AI-HPG Archive. The data format follows:

Line 1:	Date, technical specs.
Lines 2 through N:	hh mm PV_Current, PV_Voltage, Battery_Current, Battery_Voltage, Load_Current, Load_Voltage, Error msg.

With this data entry, the AI-HPG Data Flow Test #1 concluded.

Appendix B. Atmospheric Intelligence for Hybrid Power Grids (AI-HPG) Data Flow Test #2: Automating the Process

The Atmospheric Intelligence for Hybrid Power Grids (AI-HPG) Data Flow Test #2 was subdivided into two parts: a single Clear Sky Case, and a sequence of multiple Overcast Cases. The flow of data was predefined as follows:

1. Acquire measured data (Panel T, Whole Sky Imager [WSI]).
2. Calculate current and future solar radiation (SR) for a 24-h period.
3. Convert measured and forecasted atmospheric values into photovoltaic (PV) power generation.
4. Generate an optimal power grid solution.
5. Implement that optimal solution and sample the actual current/voltages for PV, battery, and load to determine the true power generated for the given time interval.

Complying with 2019 Corona Virus Infectious Disease (COVID-19) restrictions, the AI-HPG Archives were used as a resource for real-world data. The predefined time interval was 15 min for the sampled data. Due to the use of archived data separated by 15 min the automating routine advanced the cycle after a 4-min actual time period. Images were manually updated into the cue.

The following summarizes each of the cases executed in Data Flow Test #2.

B.1 Atmospheric Intelligence for Hybrid Power Grids (AI-HPG) Data Flow Test #2a (Single Image, Clear Sky Case)

Single Image: Automated_Executive Script. Once all system elements reported "go" conditions, the Test was initiated using the automating script, *df_testX_200730.m*. The single image test was completed within approximately 1 min.

Single Image: Atmospheric Intelligence to Power Optimization

Data Input. The input data files included

1) the Clear Sky WSI Image from 2019 August 16, **1200** Mountain Time (MT) (AIHPG_image_20190816_1200.png); and
2) two Panel Temperature files from the same date

   (2019 August 16, 0000–**1200 MT**; *AIHPG_panelT_20190816_full.txt*) and the previous day (2019 August 15, 0500–2059 MT; *AIHPG_panelT_20190815_full.txt*).

Data Processing. The executive script called each element's model (with the supportive files), including the following:

- WSI Image Analysis: *predict_clouds.v14.py*
- SR Model: *ShapiroAIHPG.m*
- Power Conversion: *PanelModelClass.m*
- Optimization Code: viscousClass.m, which ran the emsClass.m on the server.

Output. While individual programs generated files for posttest analyses, the executive script created run files with a name format of <*YYYYMMDD_matlabtime_descriptive.dat*>. These files included the following:

1) Sky Analysis 20200730_xxxxxx_Cloud.dat
2) Solar Radiation for 24 h 20200730_xxxxxx_SR.dat
3) Panel T for 24 h 20200730_xxxxxx_PanelTemp.dat
4) Calculated PV for 24 h 20200730_xxxxxx_PVAvail.dat
5) Pre-set Load for 24 h 20200730_xxxxxx_LoadProfile.dat
6) State of Charge 20200730_xxxxxx_StateOfCharge.dat – I/O file
7) Various System Specs 20200730_xxxxxx_Metadata.dat
8) Optimization Solution 20200730_xxxxxx_GenSetSoln.dat

Single Image: Clear Sky Case – Results. The single image Clear Sky Case results showed a successful data flow test from data input through the optimization solution steps. The numerical results had room for improvement. In a separate test, the AI-HPG Test-bed Emulator brought the solution into an emulated test-bed, simulating setting changing to the load/state of charge (SoC).

B.2 AI-HPG, Data Flow Test #2c (Multiple Images, Overcast Cases)

Multiple Images: Automated Script. Once all system elements reported "go" conditions, the four 15-min iterations, each representing 1 sample/15-min, were executed. The processing of each input (1 image/iteration) took approximately 1–2 min.

Multiple Images: Atmospheric Intelligence to Power Optimization

Single Image: Atmospheric Intelligence to Power Optimization Data Input. A sequence of four Overcast Cases from the AI-HPG Archive was used as data input. These included the following:

- Iteration 1, WSI Image: 2019 Aug 19, **1245 MT** (*AIHPG_image_20190816_1245.png*);
- Panel T: 2019 Aug 18, 0500-2059 MT (*AIHPG_panelT_20190918_full.txt*);
  2019 Aug 19, 0000-**1245 MT** (*AIHPG_panelT_20190919_full.txt*).
- Iteration 2, WSI Image: 2019 Aug 19, **1300 MT** (*AIHPG_image_20190816_1300.png*);
- Panel T: 2019 Aug 18, 0500-2059 MT (*AIHPG_panelT_20190918_full.txt*);
  2019 Aug 19, 0000-**1300 MT** (*AIHPG_panelT_20190919_full.txt*).
- Iteration 3, WSI Image: 2019 Aug 19, **1315 MT** (*AIHPG_image_20190816_1315.png*);
- Panel T: 2019 Aug 18, 0500-2059 MT (*AIHPG_panelT_20190918_full.txt*);
  2019 Aug 19, 0000-**1315 MT** (*AIHPG_panelT_20190919_full.txt*).
- Iteration 4, WSI Image: 2019 Aug 19, **1330 MT** (*AIHPG_image_20190816_1330.png*);
- Panel T: 2019 Aug 18, 0500-2059 MT (*AIHPG_panelT_20190918_full.txt*);
  2019 Aug 19, 0000-**1330 MT** (*AIHPG_panelT_20190919_full.txt*).

Data Processing. No program changes from the Clear Sky Case were made for the multiple iteration test.

Output. The executive script and program output formats were consistent with the first test.

Multiple Images/Overcast Cases: Results. A raw, first cut of the results from the multiple image Overcast Cases was reviewed. Samples of these raw data time series are shown in Figs. B-1 through B-4.

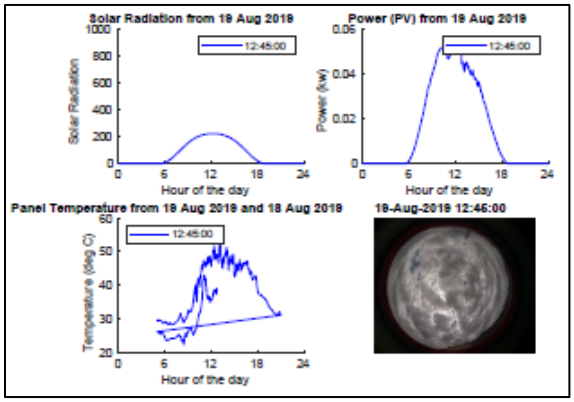

Fig. B-1 AI-HPG Data Flow Test #2c results for 2019 August 19, 1245 MT

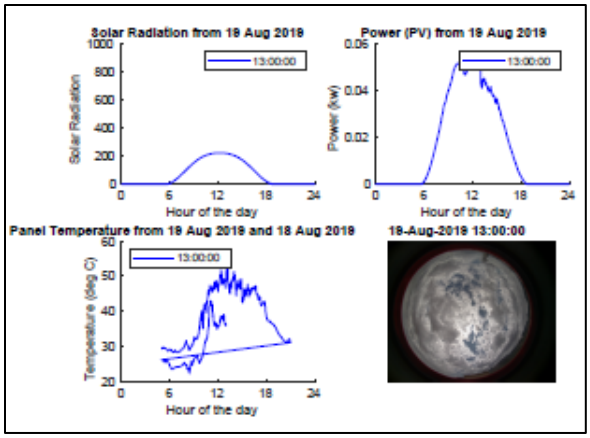

Fig. B-2 AI-HPG Data Flow Test #2c results for 2019 August 19, 1300 MT

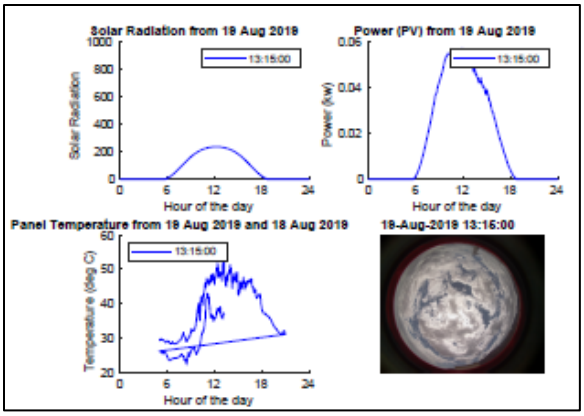

Fig. B-3 AI-HPG Data Flow Test #2c results for 2019 August 19, 1315 MT

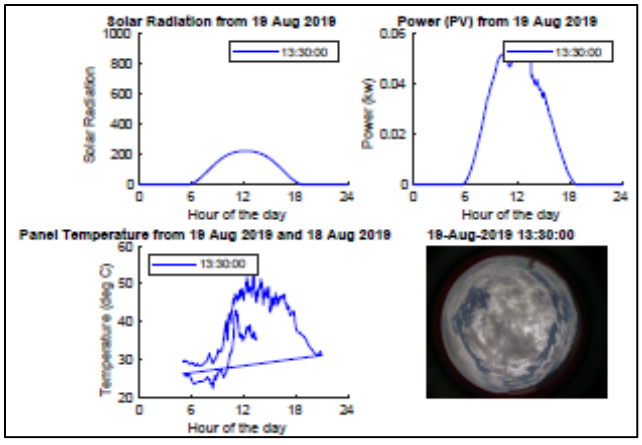

Fig. B-4 AI-HPG Data Flow Test #2c results for 2019 August 19, 1330 MT

List of Symbols, Abbreviations, and Acronyms

AI	Artificial Intelligence
AI-HPG	Atmospheric Intelligence for Hybrid Power Grids (a non-automated version of the Automated In-situ AI-HPG System)
CNN	Convolutional Neural Network
COVID-19	2019 Corona Virus Infectious Disease
EMS	Energy Management System
GA	Genetic Algorithm
GUI	graphical user interface
HVAC	heating, ventilation and air-conditioning
I	current
IPR	Internal Project Review
LT	Local Time
MDO	Multi-Doman Operations
ML	Machine Learning
MPC	Model Predictive Control
MT	Mountain Time
MTU	Michigan Technological University
MPPT	maximum power point tracking
M-X-Z	Mahmoud, Xiao, and Zeineldin
PV	photovoltaic
SoC	state of charge
SR	solar radiation
WSI	Whole Sky Imager
V	voltage

1 (PDF) DEFENSE TECHNICAL INFORMATION CTR DTIC OCA

1 (PDF) CCDC ARL FCDD RLD DCI TECH LIB

1 (PDF) ATEC B THOMAS

1 (PDF) MTU G PARKER

1 (PDF) WEST POINT C JAMES

1 (PDF) C5ISR M BAILEY

1 (PDF) GVSC D RIZZO

22 (12 PDF, 5 HC, 5 CD) CCDC ARL FCDD RLC E B MCCALL T JAMESON FCDD RLC ED G VAUCHER (5 CD, 5 HC) C HOCUT R BRICE R RANDALL M LEE M S DARCY J RABY FCDD RLS RP M BERMAN B GEIL R JANE